Adsorption of nitro-substituted aromatics on single-walled carbon nanotubes

E. S. Alldredge, Ş. C. Bădescu,* N. Bajwa, F. K. Perkins, E. S. Snow, and T. L. Reinecke
Naval Research Laboratory, Washington, DC 20375, USA
(Received 19 May 2010; published 9 September 2010)

Molecular adsorption of nitroaromatic molecules on single-walled carbon nanotubes (NTs) was investigated using state-of-the-art *ab initio* calculations and conductivity measurements. In the calculations we considered both armchair and zigzag NTs of several diameters and treated adsorption both on pristine sidewalls and oxygenated defects. The resulting adsorption energies on the pristine sidewalls were found to increase linearly with the number of NO_2 groups and with the NT diameter. The adsorption mechanism is predominantly physisorption through π-π stacking, with additional contributions from the NO_2 groups. The calculated adsorption energies at oxygenated defects were found to be comparable with those on the pristine sidewall. In both cases the functional groups give rise to local electronic polarization and to shifts in vibrational lines due to small charge transfers. The dependence of adsorption energies on the number of NO_2 groups was found to be consistent with conductivity measurements on NT arrays exposed to trace amounts of nitroaromatic derivatives.

DOI: 10.1103/PhysRevB.82.125418 PACS number(s): 73.22.−f, 81.07.De, 85.35.Kt, 68.43.−h

I. INTRODUCTION

The remarkable electronic and structural characteristics of single-wall carbon nanotubes[1] (NTs) are attracting much research effort to elucidate their properties and to develop applications based on them. Molecular sensing is based on the large surface-to-volume ratio of NTs that provides an efficient transduction channel from chemical to electrical properties even for very small amounts of adsorbates. The interactions driving the molecular adsorption are specific to each class of adsorbates, ranging from chemisorption to physisorption via weak dispersive forces, and understanding their microscopic details requires accurate theoretical tools.

Organic aromatic derivatives are particularly important for their interaction with NTs. They are involved in the binding of proteins and DNA bases to NTs,[2] in the interaction of toxic hydrocarbon species or solvents with NTs,[3,4] in monolayer assemblies on surfaces,[5,6] and in the chemical sensing[7–9] of low traces of explosives. For these adsorbates the common feature is the dispersive interaction between the molecular π orbitals and the extended π Bloch states of the NTs. This gives a weak interaction that leads to stacking in flat configurations of the molecules on the pristine sidewalls[10,11] and which can be increased by the presence of substitutional groups in the molecule or by defects in the NT.[12–14] Accurate theoretical descriptions of weak interactions require state-of-the-art first-principles methods that overcome the limitations of early density-functional treatments.[15]

In this work we focused on a quantitative understanding of interactions between nitrobenzene and nitrotoluene aromatics and NTs. They are building blocks for explosives, and understanding their adsorption is important for designing NT or carbon-material sensors for them. The cases of single benzene ring with a varying number (n=0–3) of nitrofunctional groups NO_2 can provide basic theoretical information and n is a simple parameter for standard experiments. We chose to study the following isomers: nitrobenzene, 1,3-dinitrobenzene and 1,3,5-trinitrobenzene. The nitrotoluenes have an additional CH_3 group, and the isomers considered here are toluene, 2-nitrotoluene, 2,4-dinitrotoluene, and 2,4,6-trinitrotoluene. We studied the adsorption of these molecules on pristine regions of NTs and at oxygenated defects. We found that the calculated adsorption energies increase linearly with the number of NO_2 groups for adsorption both on pristine regions and at oxygenated defects, and that the adsorption energies at oxygenated defects are comparable to but larger than those on the pristine regions. We have made also conductivity measurements of NT networks in response to trace vapors of nitroaromatics. The experimental results were consistent with the calculations, suggesting a linear dependence of adsorption energy on, and an increase in conductivity response with, the number of NO_2 groups on the molecules.

The approach use here was similar to that in Ref. 16 to study molecules of increasing size. The feature varied in Ref. 16 was the length of the linear chain in simple alkane derivatives or alkane chains with a single functional group (hydroxyl —OH or carbonyl =O). Those molecules adsorb on NTs via weak van der Waals interactions, and their adsorption energies on the pristine sidewalls were found to increase linearly with the molecular length and to be much larger at oxygenated defects. The features varied in the present work were the number of functional groups and the NT diameter. In both Ref. 16 and the present work we found that the response increased linearly with the adsorption energy and is determined mainly by molecular size. However, the dispersive forces involved in the two cases are different, namely, π-π stacking for the aromatics here vs van der Waals for the alkanes. The present work supports the view that functional groups modify the π-π stacking by polarization effects as proposed in the Hunter-Sanders model for pairs of aromatic molecules.[14]

II. CALCULATIONS

In the current calculations we used the NWCHEM code.[17] Our approach used localized basis sets of electronic func-

tions, and it incorporates recent density functionals appropriate for noncovalent bonds. We chose three representative armchair nanotubes NT(n,n) with n=5, 7, and 9, and three representative zigzag nanotubes NT(n,0) with n=8, 11, and 14. These give a range of diameters from 0.63 to 1.22 nm. The optimized geometries of NTs were obtained using periodic boundary calculations. These structures were then cut to finite-length clusters terminated with hydrogen atoms and were used to treat the adsorption. We used the ONIOM technique[18] to split the system into two regions, each treated self-consistently with different chemical accuracies. The chemically relevant region in the center contained the adsorbed molecule and a large region with 14 carbon rings underneath it. This region was treated using the meta-generalized gradient approximation hybrid density functional M05-2X (Ref. 19) with the 6-31G(d,p) polarized basis.[17] This functional has been designed to treat weak noncovalent interactions between molecules.[20] The remote environment is used to obtain accurate electronic boundary conditions on the cluster and is described with the minimal Gaussian STO-2G basis.[17] To verify the accuracy of the ONIOM approximation used, in the case of nitrotoluene we compare with the full density-functional theory (DFT) results for the zigzag NTs n=5, n=9 and on the armchair NTs n=8, n=14. For all test cases the full-DFT adsorption energy is larger by 5–10 meV, associated to the boundary conditions of the DFT layer. This consistent deviation is much smaller than the absolute adsorption energy, therefore we used the more economical ONIOM method to obtain the results reported below.

Structural relaxation of each molecule is obtained by minimizing of the total energy $E_{\mathrm{NT+mol}}$ of the molecule and NT system. For adsorption on the pristine sidewalls the NT is frozen and the coordinates of the adsorbed molecule are relaxed. For NTs with defects the atoms in the defect are relaxed along with those of the molecule. For pristine graphene we used a frozen sheet containing 42 C atoms with 16 H atoms saturating the edges (a size similar to the DFT layer used in the NTs). The adsorption energy is determined by $E_{ads}=E_{\mathrm{NT+mol}}-(E_{\mathrm{NT}}+E_{\mathrm{mol}})$, where E_{NT} is the energy of the pristine NT or of the NT with the relaxed defect, E_{mol} is the energy of the free-relaxed molecule.

The constraints used in the optimization are validated by comparing with the full-DFT cases mentioned above. In the presence of nitrotoluene the full DFT, unconstrained, relaxation of a pristine NT adds to E_{ads} less than 5 meV without any observable deformation of the NT. The full DFT, unconstrained relaxation of a NT with a carboxyl defect in the presence of nitrotoluene leads to the same deformation of the defect as the ONIOM calculation, without any significant relaxation of the remote C atoms and with the same perturbation to E_{ads}. These small deformations are understood by noticing that the C atoms are bonded by strong sp^2 bonds, which are not affected by the adsorbates, as discussed further in the paper. Constraining most of the C atoms in the NT is more economical and avoids unphysical deformations of the high-level layer due to boundary conditions in the ONIOM description.

A. Adsorption on pristine NT sidewalls

First we discuss adsorption on the defect-free NT sidewall. Calculated adsorption energies E_{ads} for nitrotoluenes and nitrobenzenes on armchair and zigzag NT sidewalls are shown in Figs. 1 and 2 as a function of the number n of nitro groups. These were found to range from below 200 meV to above 500 meV and are characteristic of noncovalent bonds. The optimal adsorption configurations for nitroaromatics on pristine sidewalls are found to have the carbon rings lying flat above the NT surface. This gives the largest contribution to E_{ads} (corresponding to the energy of ≈250 meV for benzene), which is associated mainly with the π-π stacking of the aromatic ring and the NTs. Each additional NO_2 functional group increases E_{ads} uniformly leading to an almost linear dependence on the number n of NO_2 groups both for nitrotoluenes and nitrobenzenes (Fig. 1). Adsorption energies for both types of molecules are also found to increase monotonically with the NT size over the range of NTs investigated (0.63–1.22 nm, Fig. 1). Comparisons between E_{ads} for the nitrotoluene and the nitrobenzene series are shown in Fig. 2(a) for an armchair nanotube NT(5,5) and in Fig. 2(b) for a zigzag nanotube NT(8,0). The calculated incremental adsorption energies $\Delta E_{\mathrm{NO_2}}$ per NO_2 group for the two nitroaromatic groups on different NTs are given in Table I.

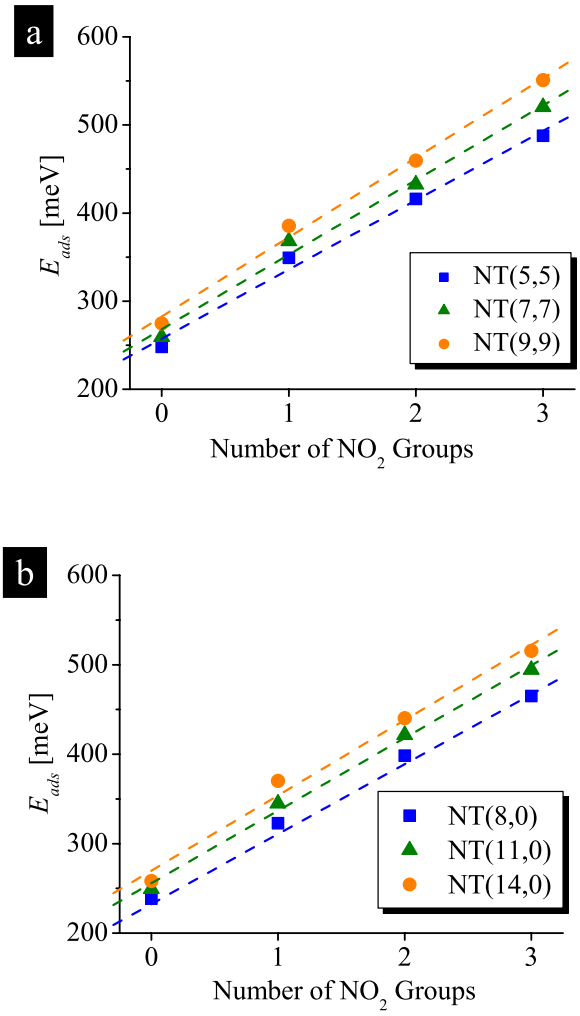

FIG. 1. (Color online) Calculated adsorption energies E_{ads} for the nitrotoluene series from toluene (n=0) to trinitrotoluene (n=3) on (a) armchair NTs and (b) zigzag NTs.

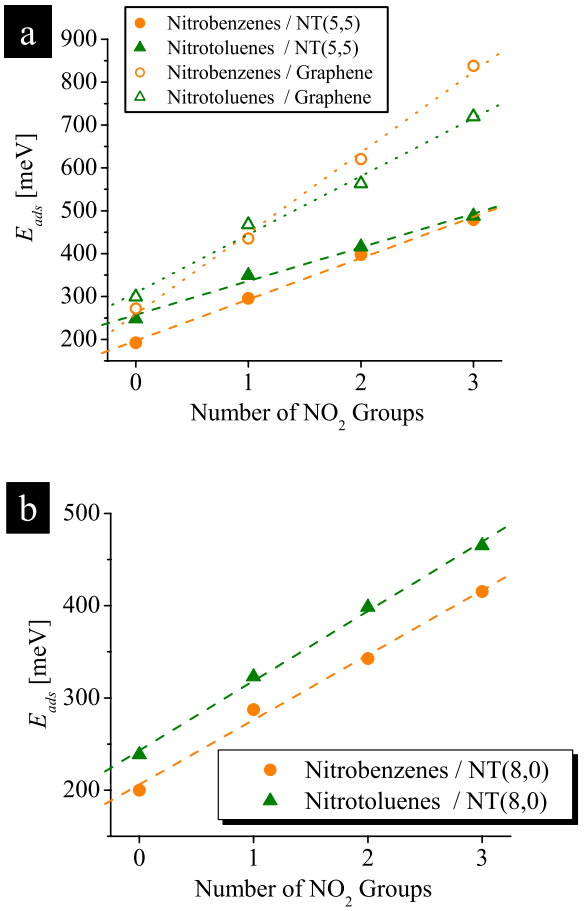

FIG. 2. (Color online) Comparison of calculated adsorption energies E_{ads} for the nitrotoluene and nitrobenzene series at pristine areas of (a) NT(5,5) and graphene and (b) NT(8,0). Linear fits to the data yield the slopes in Table I.

We do not observe the formation of shared orbitals typical of chemisorption for either nitrobenzenes or nitrotoluenes. Mulliken charge analysis gives very small charge transfers between the molecules and NTs (typically less than $0.1e$) characteristic of physisorption. The interactions of the functional groups with the surface are due mainly to the interaction between the molecular dipoles and their images induced in the NT. The latter are observed as a charge redistributions within the surface of the NT, on the order of 0.2 e for the C atoms beneath the NO_2 groups.

Figures 3(a) and 3(b) show examples of optimal adsorption geometries of nitroaromatics on selected pristine NTs. For all the molecules considered here the optimal positions of the benzene rings are aligned with a high-symmetry C—C bond (transversal to the axis for armchair and axial for zigzag NTs). Aligning the benzene ring with the other C—C bonds in the NT decreases the adsorption energies by as much as 40 meV. For 2-nitrotoluene and 2,4-dinitrotoluene, the NO_2 group next to CH_3 ends in a symmetric position (along a C—C bond), pushing the CH_3 group into an asymmetric orientation (at an angle $\pi/6$ from the axis on the armchair NTs and $\pi/3$ on zigzag NTs). For 2,4,6-trinitrotoluene the optimal configuration has both the CH_3 group and the opposite NO_2 group aligned with a C—C bond, as shown in Figs. 3(a) and 3(b). In all these cases, the positions obtained by $\pi/3$ around the center of the benzene ring are metastable, with adsorption energies smaller by $\approx$30 meV and isolated by energy barriers larger than 100 meV.

For adsorption on armchair NTs, the aromatic ring is found to be centered over the C—C bonds of the NT (bridge configuration) while for zigzag NTs the aromatic rings are centered over a single carbon atom of the NT (top configuration). This helps us to understand the difference between the slopes of adsorption energies on the armchair NTs and on zigzag NTs (Fig. 2). For armchair NTs [Figs. 2(a) and 3(a)] the presence of CH_3 in the nitrotoluenes prohibits them from getting as close to the NT as the nitrobenzenes, which can settle in an optimal configuration parallel to NTs. Therefore the adsorption at the bridge site on the armchair NTs results in larger values of $\Delta E_{ads}^{NO_2}$ for the nitrobenzene series than for the nitrotoluene series. In contrast, on zigzag NTs [Figs. 2(b) and 3(b)] both nitrobenzenes and nitrotoluenes assume similar planar orientations and therefore their rates of increase in the adsorption energies $\Delta E_{ads}^{NO_2}$ with the number of NO_2 in Table I are similar. For the zigzag NTs the difference between the two classes is approximately a constant associated with the CH_3 of the nitrotoluenes.

We now turn to the monotonic increase in the adsorption energies with the size of NTs. This is due to the reduction in curvature which brings more of the NT into interaction with the adsorbate. This results in an increase in the adsorption energy with number of NO_2 groups that is significantly larger for nitrobenzenes than for nitrotoluenes [Fig. 2(a)]. Again, this is due to the CH_3 group which pushes the molecule slightly off the NT adsorption site. The effect of NT curvature on the interaction energy for NTs can be seen in the larger values of $\Delta E_{ads}^{NO_2}$ for larger NTs in Table I, with the largest values occurring for graphene. In the limiting case of graphene (zero curvature) we find that adsorption occurs in the bridge orientation, similar to Fig. 3(a). For molecules on NTs of small diameter, the NO_2 groups lie farther away from the NT, yet they contribute in the same way to give linear increases in the adsorption energies. Our calculations are

TABLE I. Calculated values of the slope $\Delta E_{ads}^{NO_2}$ of the adsorption energy in meV versus the number n of NO_2 groups for nitrobenzenes and nitrotoluenes on pristine NTs and graphene.

	NT(8,0)	NT(11,0)	NT(14,0)	NT(5,5)	NT(7,7)	NT(9,9)	Graphene
Diameter (nm)	0.63	0.86	1.10	0.68	0.95	1.22	∞
$\Delta E_{\text{benzene}}^{NO_2}$	70	77	88	96	108	114	188
$\Delta E_{\text{toluene}}^{NO_2}$	76	81	84	79	89	91	136

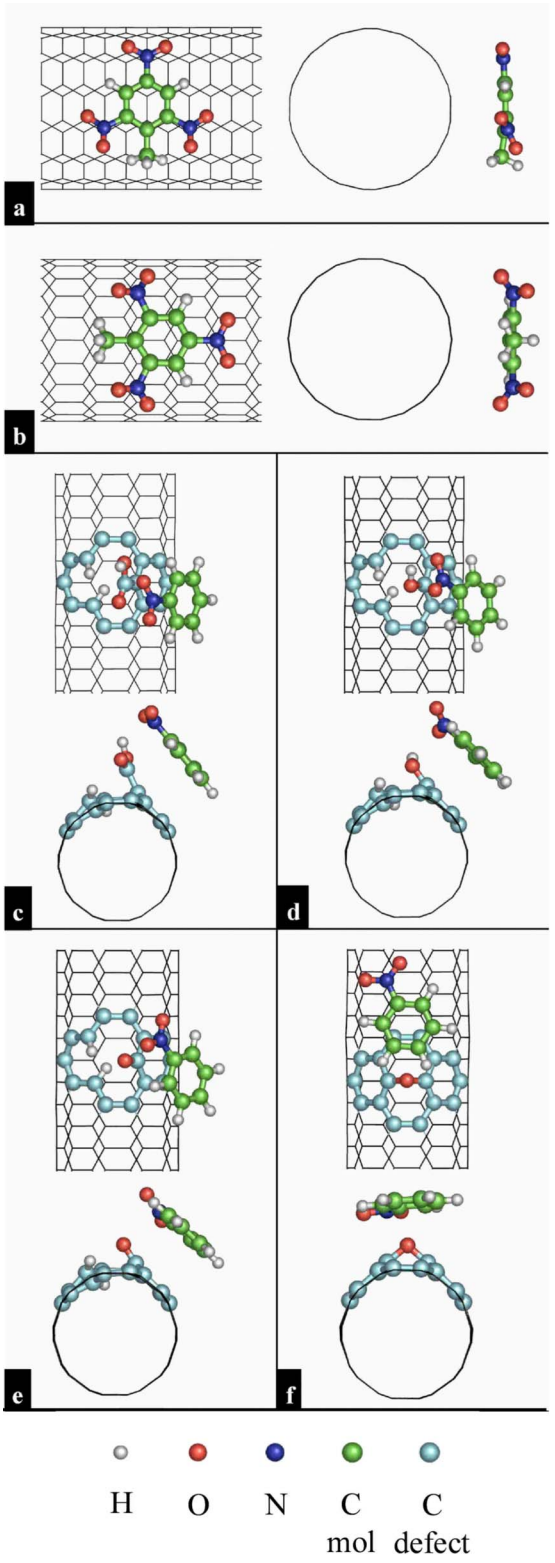

FIG. 3. (Color online) [(a) and (b)] Trinitrotoluene adsorbed on pristine NTs, with top and axial views: (a) armchair NT(7,7) and (b) zigzag NT(11,0). Nitrobenzene adsorbed at oxidation defect in NT(5,5): (c) carboxyl defect —COOH, (d) hydroxyl defect —OH, (e) carbonyl defect =O, and (f) epoxy defect C—O—C. Carbon atoms of the adsorbate are green, nitrogen atoms are blue, oxygen atoms are red, and hydrogen atoms are white. The carbon atoms around the NT defect are light blue.

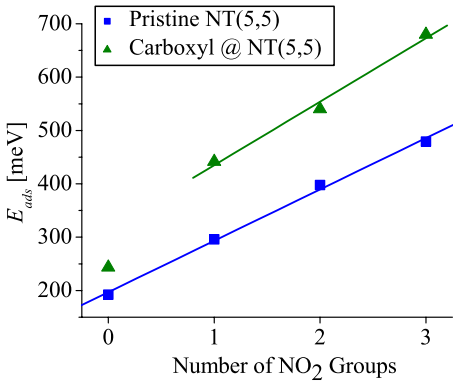

FIG. 4. (Color online) Calculated adsorption energies E_{ads} for nitrobenzenes at a carboxyl defect compared to adsorption at pristine areas of a NT(5,5). Here, $n=0$ represents benzene and $n=3$ represents trinitrotoluene.

consistent with the Hunter-Sanders model[14,21,22] in which the functional groups contribute with attractive σ-π interactions to overcome the repulsive π-π interaction between the molecular and NT orbitals. The functional groups have a mostly electrostatic effect and they determine the adsorption geometry while the largest part of the adsorption energy is determined by the dispersive forces.

B. Adsorption at defects

NTs typically can contain defects produced in the fabrication process or introduced to increase their sensitivity to polar molecules. Previous work[8] showed that oxygenation defects from ozonization can change the conductance response of NTs and increase their sensitivity to molecular adsorbates by up to an order of magnitude. This has been attributed to larger binding energies for adsorbates at the defect sites and to charge transfer.[8] To determine whether such defects are important for nitroaromatics, we have performed calculations of the adsorption energies of nitrobenzenes at the dominant oxygen-related defects in NTs, namely, the carboxyl —COOH, hydroxyl —OH, carbonyl =O, and epoxy C—O—C [Figs. 3(c)–3(f)].

Due to geometrical constraints only one NO_2 group in each molecule can interact significantly with a defect, and additional NO_2 groups attached to nitrobenzene interact primarily with the NT sidewall away from the defect. The result is a rate of increase in E_{ads} with the number of NO_2 groups similar to that on pristine sidewalls. This behavior is shown in Fig. 4 for adsorption at a carboxyl defect. In the following we focused on nitrobenzene ($n=1$) since it is the simplest of the nitroaromatics.

The optimized adsorption configurations for nitrobenzene at the oxygenated defects of a NT(5,5) are shown in Figs. 3(c)–3(f) and the calculated E_{ads} are given in Table II. We found that the defects with an —OH group (carboxyl and hydroxyl) give larger adsorption energies than pristine regions NTs. This results primarily from the interaction between the NO_2 group of nitroaromatics and —OH of the defect, which determines the most probable adsorption configurations in Figs. 3(c) and 3(d). Although relatively large,

TABLE II. Calculated adsorption energies E_{ads} (in meV) of aromatic molecules with no functional group (benzene), an OH functional group (benzenol), and an NO_2 group (nitrobenzene) at oxygenated defects in NT(5,5).

	Pristine	Carboxyl	Hydroxyl	Carbonyl	Epoxy
Benzene	192	243	252	215	171
Benzenol	254	579	311	550	408
Nitrobenzene	296	454	381	284	295

this interaction is not strong enough to reorient the benzene ring of the molecule away from the NT surface. Therefore this interaction adds to the π-π stacking between the benzene ring and pristine regions of the NT near the defect, yielding adsorption energies larger than those for nitrobenzene on pristine NTs (Table II).

We found that the defects that do not contain a hydroxyl group, namely, carbonyl ═O and epoxy C—O—C [Figs. 3(e) and 3(f)] gave a weaker adsorption energies for nitrobenzene. For the epoxy defect, the NO_2 group is repelled by the defect and the opposite hydrogen on the ring is slightly attracted by it [Fig. 3(e)]. This configuration is nearly the same as that of adsorption on the pristine NT and gives a similar E_{ads}, as shown in Table II. If the NO_2 group is positioned near the epoxy defect, a E_{ads} more than 50 meV lower than that on a pristine NT(5,5) was obtained. At the carbonyl defect, a configuration with the NO_2 group near the defect [Fig. 3(f)] was found to have an adsorption energy slightly smaller than in the case of the pristine NT.

We compared the adsorption of nitrobenzene at defects to that of two other molecules. First we considered benzene and used it as a reference ($n=0$); we found that benzene does not interact strongly with any of the defects considered here, giving only an additional $\approx$50 meV to E_{ads} at carboxyl and carbonyl defects compared to the pristine sidewall, and suggesting that the binding is increased by NT defects only for molecules with polar functional groups. The second molecule used for comparison was benzenol. It was found that the functional group —OH of benzenol increases the adsorption energies at oxygenated defects for other molecules that carry this group, e.g., linear molecules studied theoretically and experimentally in Ref. 16. Also, the response to benzenol itself was measured in Ref. 8. In addition, it was shown theoretically that increasing the number of —OH groups attached to benzene gives an almost linear increase in the adsorption energy[13] with a slope larger to the present one for nitrobenzenes. The present results on benzenol are given in Table II. In contrast to benzene, the —OH group forms a strong hydrogen bond with the defects, with an additional $\approx$300 meV compared to E_{ads} on pristine sidewalls. Benzenol is found to adsorb more strongly than nitrobenzene at all oxygenation defects considered here, except the hydroxyl defect.

The NT conductivity response to adsorbates depends on the adsorbate residence time on the surface and on changes induced by adsorbates, such as charge transfer, polarizations, and scattering. The residence time is determined by the adsorption energy, and it scales as e^{E_{ads}/k_BT} for a temperature T. The increased E_{ads} at defects as compared to the pristine NT surface are modest for nitrobenzene, less than 100 meV at the hydroxyl and about 150 meV for the carboxyl defects. However, the ratio of the residence times can be more than an order of magnitude. These increased residence times at defect sites are consistent with large changes in the conductivity responses seen in measurements of adsorbates, including aromatics on oxidized NTs.[8]

The standard description of charge rearrangements in *ab initio* calculations uses the so-called Mulliken charge. This represents the integrated electronic charge within a set of spherical regions centered on selected atoms. The change in Mulliken charge is a good approximation for covalent and strongly ionic bonds. In the case of physisorption this integral can miss the local charge polarization next to each atom. Here, the calculated changes in the Mulliken charge of the molecule are small ($<0.1e$) and cannot account for large variations in NT conductivity, suggesting only a charge polarization around the molecule. These values cannot describe accurately the charge redistribution between orbitals, and in order to gain more insight we have to consider other charge effects.

C. Shifts of molecular vibrational lines

An alternative approach for learning about charge effects is to analyze the shifts of molecular vibrational modes since small orbital hybridization can strengthen or weaken bonds. First we performed *ab initio* calculations of the shifts of IR modes of nitrobenzene on pristine NT sidewalls and at oxygenated defects. The most active IR modes of nitrobenzene are a C—N stretch mode at $\nu^{s1}_{C—NO_2}=895$ cm^{-1} in which the NO_2 group has a "scissor" vibration, a symmetric C—NO_2 mode at $\nu^{s2}_{C—NO_2}=1500$ cm^{-1} in which the N—O bonds have a "stretch" vibration, and the asymmetric N—O stretch vibrations at $\nu^{a1}_{N—O}=1710$ and $\nu^{a2}_{N—O}=1774$ cm^{-1}. Upon adsorption on pristine NTs $\nu^{s1}_{C—NO_2}$ is not shifted significantly but it losses intensity. The symmetric mode $\nu^{s2}_{C—NO_2}$ is redshifted by $\delta\nu^{s}_{C—NO_2}\approx -5$ meV. The largest redshifts on pristine NTs are observed for the asymmetric modes, $\Delta\nu^{a1}_{N—O}=-8$ and $\Delta\nu^{a2}_{N—O}=-12$ cm^{-1}. This can be explained by inspecting the lowest unoccupied molecular orbital (LUMO) of the molecule, which has an antibonding character between the N and O atoms; a redshift of the N—O stretch mode is consistent with a small charge addition to this orbital. This occurs by the hybridization of the molecular LUMO with the NT orbitals, leading to a decrease in the gap between the lowest occupied molecular orbital (HOMO) and the LUMO by 1.6 eV. This hybridization is responsible for the localiza-

tion of a small electronic charge of the NT next to the molecule. As a consequence the density of p carriers in the NT increases and the conductivity of the originally p-doped NT increases. When this molecule is adsorbed at the hydroxyl or carboxyl defects the symmetric C—NO_2 stretch mode is redshifted from $\nu^{s2}_{C—NO_2}=1500$ cm^{-1} to 1495 cm^{-1} due to the interaction with the polar defect; the N—O stretch modes are redshifted at the hydroxyl and carboxyl defects by $\Delta\nu^{a1}_{N—O}=-8$ and $\Delta\nu^{a2}_{N—O}=-17$ cm^{-1}. In these cases the hybridization of the LUMO with NT orbitals is stronger due to defect states, leading to a larger decrease in the molecular HOMO-LUMO gap. No significant shifts are observed for geometries with the nitro group next to epoxy or carbonyl defects. The redshifts mentioned here do not depend significantly on the size of the NT, supporting the picture of local polarization of the electron charge toward the molecule.

Next we considered toluene and made a similar analysis. The changes in the vibrational lines of the methyl functional group CH_3 upon adsorption on the NTs were found to be very small. This is due to the lack of a significant bond polarization of the methyl group: the HOMO-LUMO gap of toluene changes by less than 0.5 eV. In this case the charge localization next to the molecule was much weaker, and this molecule would change the conductivity mainly by decreasing the scattering.

Finally, we considered the influence of the number of functional groups in the adsorbed molecules on their vibrational frequencies, by considering the case on trinitrobenzene. The largest shift occurs in the asymmetric N—O stretch modes, which are shifted from $\nu^{a1}_{N—O}=1789$ cm^{-1} and $\nu^{a2}_{N—O}=1791$ cm^{-1} by $\Delta\nu^{a1}_{N—O}=-9$ cm^{-1} and $\Delta\nu^{a2}_{N—O}=-8$ cm^{-1}. These are comparable with the redshifts for nitrobenzene adsorbed on NTs, which shows that the charge polarization is roughly the same for all of the NO_2 groups in the molecule.

Previous experimental works considered the reverse effect, namely, the change in vibrational properties of NTs by charge polarizations induced by nitrobenzene.[23] To observe vibrational shifts via Raman spectroscopy the NTs had to be covered with many nitrobenzene molecules from solution.[23] The mechanism of mutual polarization NT molecule giving the band shifts in Ref. 23 is also responsible for the present molecular line shifts.

III. EXPERIMENT

We performed measurements of the conductance responses of NT-network sensors to the adsorption of nitroaromatic gases. We used random NT networks fabricated by chemical vapor deposition on a 30-nm-thick thermal oxide layer on a 0.001 Ω cm silicon substrate. Using standard photolithography and lift-off and etching techniques, an interdigitated array of Ti/Au electrodes was deposited on top of each NT network. These procedures had been described earlier.[7,24] Although there is no intentional oxygenation of these arrays, we expect some oxidized defects to be present. The conductance G of the NT network is measured with a lock-in amplifier, tuning the ac bias voltage at 700 Hz to maintain a current of 5 μA across the sensor. Dilute vapors

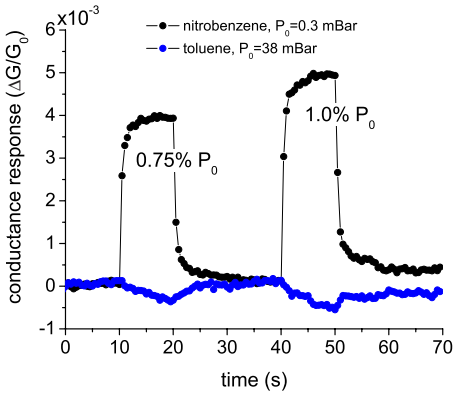

FIG. 5. (Color online) Normalized conductivity $\Delta G/G_0$ in ambient conditions for NT arrays upon exposure to timed pulses of nitrobenzene and toluene vapor at two concentrations. G_0 is the conductance of the array in the absence of vapor.

are delivered to the sensors by bubbling a low flow of dry air through liquid nitrotoluenes and mixing this saturated vapor with a high flow of dry air.

Figure 5 shows typical responses for the relative conductance changes $\Delta G/G_0$ of a NT array for low vapor pulses of nitrobenzene and toluene at room temperature. It can be seen that the conductivity increases upon adsorption of nitrobenzene whereas it decreases for toluene. This suggests that for nitrobenzene local polarizations due to adsorbate-induced charges dominate over scattering, whereas toluene changes the conductivity mainly by scattering. Using a simple kinetic model,[16] we take the NT conductance change to be proportional to the adsorbate population on the NT surface and to the perturbation g induced by a single molecule,

$$\Delta G/G_0 \propto \Phi \cdot \tau \cdot g(\Delta\mu, \Delta Q). \tag{1}$$

Here Φ is the molecular flux and τ is the average residence time of the adsorbate. g includes the effects of scattering on the mobility μ and of charge transfer ΔQ on the carrier density. The residence time is taken to have the form of a Boltzmann factor $\tau \propto e^{E_{exp}/k_BT}$, where E_{exp} represents the adsorption energy and T is the room temperature. To determine the dependence of E_{exp} on the number of NO_2 groups n we fix a value of the response $\Delta G/G_0$ and determine the molecular flux Φ for that response as a function of n. From $\Phi|_{\Delta G/G_0} \propto 1/\tau g$ we obtain

$$\ln(\Phi)|_{\Delta G/G_0} = \text{const} - \frac{E_{exp}}{k_BT} - \ln g. \tag{2}$$

Values of $\ln(\Phi)|_{\Delta G/G_0}$ determined in this way are shown as a function of n in Fig. 6, where the dependence of $\ln(\Phi)$ on n is roughly linear. In the lowest order we can take the dominant dependence on n in Eq. (2) from the adsorption energy with the form $E_{exp} \approx E_0 + n \times E^{NO_2}_{exp}$, with the dependence $\ln g$ on n being relatively weak. Here $E^{NO_2}_{exp}$ gives the experimental adsorption energy contributed by each of the NO_2 groups and is assumed to be the same for all NO_2 groups. This is consistent with the dependence found in the calculations. In this approximation, the measurements for the nitrotoluene series suggest an incremental adsorption energy per NO_2 group of

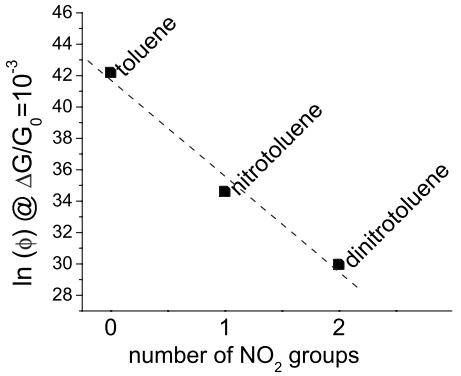

FIG. 6. Logarithm of the molecular flux (Φ) for a fixed value of the response $\Delta G/G_0$ vs the number n of NO_2 atoms in the molecule. The linear fit provides the dependence of the binding energy $E_{exp}^{NO_2}$ with n.

≈150 meV. This value is somewhat larger than the calculated values given in Table I for adsorption at pristine regions and it is closer to the slope of 120 meV calculated for nitrobenzenes at a carboxyl defect. The difference between the measured and the calculated values may also be affected by the n dependence of the total scattering and by the total charge effect of a molecule, both these effects being incorporated in g in Eq. (2). In addition, the experiments use a distribution of NT sizes.

In a previous work[16] we observed experimentally large decreases in conductance upon exposure to alcohols and ketones, which are polar molecules obtained from inert alkane chains by adding —OH and ═O groups. The ═O group of ketones has a dipole moment of ≈2.8 D and these molecules are weak electron donors. The alcohols carry a smaller dipole moment of ≈1.6 D and these molecules are strong electron donors. The large decrease in NT conductance in Ref. 16 was traced to dipolar scattering from the molecules adsorbed on pristine regions of the NT. In spite of their smaller dipole moment the alcohols induce a stronger effect than the ketones since they are electron donors, annihilating partially the p character of the NTs. In the present case the experimental increase in conductance for nitroaromatics suggests that for them the charge effects are dominating over scattering. The nitro group is known a strong electron acceptor. The calculations from the previous sections showed that the charges are only weakly polarized at the NT surface. Such local polarization effects have been predicted theoretically for graphene with localized charge impurities,[25] where they have been called "charge puddles" and the existence of which was proven later experimentally.[26,27] The local charge contained in a few-nanometer puddle was found to be on the order of $0.1e$, comparable to the charge redistributions calculated here.

IV. CONCLUSION

We have shown through *ab initio* calculations that the adsorption energies of nitroaromatic molecules on pristine NTs increase approximately linearly with the number of NO_2 groups. Oxygenated defects containing an OH group give slightly larger adsorption energies compared to adsorption on perfect sidewalls. The charge polarizations in these systems are given by small hybridizations between the molecular orbitals and the NT orbitals, and they can be observed in the shifts of vibrational lines of the molecules. The redshifts of the vibrational lines of the NO_2 group suggest a small local accumulation of electronic charge next to these groups. The current linear dependence of adsorption energies is consistent with conductivity measurements performed on arrays on NTs. In the experiments discussed here we found an increase in conductance due to the nitro groups, which is consistent with an increase in the p doping in the present calculations and suggesting that for nitroaromatics the charge effects are stronger than the scattering effects. This is opposite to the effect induced previously by alcohols derived from alkane chains, for which the effect of repelling electrons adds to dipolar scattering.[16] Other physisorbed polar molecules with low electron affinity, such as ketone derivatives, were found to change the conductivity mainly by scattering.[16] For adsorbed nitrobenzenes, the charge puddle effects on conductivity seem to be related to the Hunter-Sanders polarization mechanism[13,14,28] that gives the interaction between functionalized aromatics. The present results show that the balance between scattering and doping is specific to each functional group.

ACKNOWLEDGMENTS

This work was supported in part by ONR and DTRA. E.S.A. was a NRC Research Associate, and N.B. was an ASEE Research Associate. We acknowledge the support of the DoD High Performance Computing system for the calculations and also useful discussions with Victor M. Bermudez.

*Corresponding author; stefan.badescu@nrl.navy.mil

[1] J. Charlier, X. Blase, and S. Roche, Rev. Mod. Phys. **79**, 677 (2007).
[2] Y. Wang, J. Phys. Chem. C **112**, 14297 (2008).
[3] D. Lin and B. Xing, Environ. Sci. Technol. **42**, 7254 (2008).
[4] B. Pan and B. Xing, Environ. Sci. Technol. **42**, 9005 (2008).
[5] P. B. Paramonov, V. Coropceanu, and J.-L. Bredas, Phys. Rev. B **78**, 041403(R) (2008).
[6] W. Chen, H. Huang, A. Thye, and S. Wee, Chem. Commun. (Cambridge) 2008, 4276.
[7] E. Snow, F. Perkins, E. Houser, Ş. C. Bădescu, and T. Reinecke, Science **307**, 1942 (2005).
[8] J. Robinson, E. Snow, Ş. C. Bădescu, T. Reinecke, and F. Perkins, Nano Lett. **6**, 1747 (2006).
[9] J. Kong, N. Franklin, C. Zhou, M. Chaline, S. Peng, K. Cho, and H. Dai, Science **287**, 622 (2000).

[10] L. M. Woods, Ş. C. Bădescu, and T. L. Reinecke, Phys. Rev. B **75**, 155415 (2007).
[11] F. Tournus and J. C. Charlier, Phys. Rev. B **71**, 165421 (2005).
[12] S. Wheeler and K. Houk, J. Am. Chem. Soc. **130**, 10854 (2008).
[13] A. Rochefort and J. Wuest, Langmuir **25**, 210 (2009).
[14] C. A. Hunter and J. K. M. Sanders, J. Am. Chem. Soc. **112**, 5525 (1990).
[15] Y. Zhao and D. G. Truhlar, J. Chem. Theory Comput. **1**, 415 (2005).
[16] E. S. Alldredge, Ş. C. Bădescu, N. Bajwa, F. K. Perkins, E. S. Snow, T. L. Reinecke, J. L. Passmore, and Y. L. Chang, Phys. Rev. B **78**, 161403(R) (2008).
[17] E. J. Bylaska *et al.*, NWCHEM, A Computational Chemistry Package for Parallel Computers, Version 5.0, Pacific Northwest National Laboratory, Richland, Washington, 2006.
[18] M. Svensson, S. Humbel, R. D. J. Froese, T. Matsubara, S. Sieber, and K. Morokuma, J. Phys. Chem. **100**, 19357 (1996).
[19] Y. Zhao, N. E. Schultz, and D. G. Truhlar, J. Chem. Theory Comput. **2**, 364 (2006).
[20] Y. Zhao and D. G. Truhlar, J. Chem. Theory Comput. **3**, 289 (2007).
[21] F. Ortmann, W. G. Schmidt, and F. Bechstedt, Phys. Rev. Lett. **95**, 186101 (2005).
[22] W. G. Schmidt, K. Seino, M. Preuss, A. Hermann, F. Ortmann, and F. Bechstedt, Appl. Phys. A **85**, 387 (2006).
[23] R. Voggu, C. S. Rout, A. D. Franklin, T. S. Fisher, and C. N. R. Rao, J. Phys. Chem. C **112**, 13053 (2008).
[24] J. Robinson, E. Snow, and F. Perkins, Sens. Actuators, A **135**, 309 (2007).
[25] E. H. Hwang, S. Adam, and S. Das Sarma, Phys. Rev. Lett. **98**, 186806 (2007).
[26] J.-H. Chen, C. Jang, S. Adam, M. S. Fuhrer, E. D. Williams, and M. Ishigami, Nat. Phys. **4**, 377 (2008).
[27] Y. Zhang, V. W. Brar, C. Girit, A. Zettl, and M. F. Crommie, Nat. Phys. **5**, 722 (2009).
[28] J. Wuest and A. Rochefort, Chem. Commun. (Cambridge) 2010, 2923.